Molecular fluctuations in polyethylene melts. Dependence of the longitudinal and transverse proton relaxation on the chain length

H. Koch, R. Bachus and R. Kimmich

Sektion Kernresonanzspektroskopie, Universität Ulm, Postfach 4 066, D-7900 Ulm, Federal Republic of Germany

(Received 30 January 1980)

Melts of diverse fractions of linear polyethylene have been investigated by longitudinal and transverse proton relaxation. A three-component model of molecular fluctuations allows to describe the longitudinal relaxation times in the frequency range of our experiments (10^4 to 10^8 Hz). The components are 'anisotropic segment reorientation', 'reptation' and the 'conformational fluctuation of the surrounding tube'. The molecular weight dependences of the corresponding time parameters are $\tau_s \sim M^0$, $\tau_l \sim M^1$ and $\tau_r \sim M^3$, respectively. These quantities also permit us to explain the molecular weight dependence of the transverse relaxation curves which have been described by the aid of the Anderson–Weiss theory. It is shown that the influence of the molecular weight distribution is not negligible. Rather it is the reason for non-exponential relaxation decays. The free induction decays have been found to decrease essentially faster than the relaxation decays even if the inhomogeneity of the magnet was negligible. As an explanation, internal inhomogeneities caused by microscopic voids have been assumed. An estimate of this effect is given. In addition to the pure fractions we have also studied a mixture of short chains in a matrix of long deuterated chains. It turns out that the fluctuation of the local network depends on *both* molecular weights and the ratio of mixture.

INTRODUCTION

The molecular weight dependence of the nuclear magnetic relaxation of polymer melts has been studied various times[1-3]. It was found that this dependence is different at different frequencies. The strongest effect was observed at the low-frequency T_1 plateau[2] and for transverse relaxation[1].

A description of the molecular weight dependent relaxation behaviour was suggested[4] with the three-component model. Starting from the thermal excitation of elementary processes (segment re-arrangements caused virtually by defect displacements), two secondary processes are relevant, namely longitudinal chain diffusion or reptation[5] and the fluctuation of the local conformation of the surrounding tube (*Table* 1). Segment re-orientation is anisotropic so that the corresponding n.m.r. correlation function is reduced only to a certain residual correlation. The final decrease to zero is caused by the secondary processes. Reptation leads to a loss of the correlation to the local *chain* orientation as a consequence of the diffusion around conformational bends[7]. The conformational fluctuation causes a decrease of the correlation of local *tube* orientation[4]. Thus we use the following picture: segment reorientation is caused by defect diffusion, which leads, on the other hand, to the reptation processes. Conformational fluctuation of the surrounding tube is finally a consequence of the reptation of the entangled chains defining the local network. The effective formulae for the n.m.r. correlation and intensity functions are in the case of exponential orientation correlation functions[4]:

$$G(\tau)=\left[a_0\exp\left(-\frac{\tau}{\tau_0}\right)+a_1\exp\left(-\frac{\tau}{\tau_s}\right)+a_2\right]\exp\left(-\frac{\tau}{\tau_r}\right)\times\exp\{\tau/2\tau_l\}\quad(1-\mathrm{erf}\sqrt{\tau/2\tau_l}) \tag{1}$$

with $G(0)=1$ and $G(\infty)=0$

$$I(\omega)=\sum_{j=0}^{2}a_j\times\frac{2\tau_c^{(j)}+\tau_c^{(j)3/2}\tau_l^{-1/2}(1+K^{(j)})^{1/2}}{K^{(j)2}+\frac{1}{2}\tau_c^{(j)}\tau_l^{-1}K^{(j)}+\tau_c^{(j)1/2}\tau_l^{-1/2}[(1+K^{(j)})^{1/2}+\omega\tau_c^{(j)}(K^{(j)}-1)^{1/2}]} \tag{2}$$

respectively (compare *Table* 1).

The abbreviations are

$$K^{(j)}=\sqrt{1+(\omega\tau_c^{(j)})^2}$$

$$\tau_c^{(0)}\approx\tau_0$$

$$\tau_c^{(1)}\approx\tau_s$$

$$\tau_c^{(2)}=\tau_r$$

0032-3861/80/091009-08$02.00

Table 1 Components of molecular fluctuations in polymer melts

Component	Characteristic time constant(s)	Relative amplitude(s)	Molecular weight dependence	Individual correlation function(s)
Anisotropic segment re-orientation	τ_0, τ_s	a_0, a_1	$\sim M^0$	$\exp(-\tau/\tau_{0,s})$
Longitudinal chain diffusion (reptation)	τ_l	a_2	$\sim M^1$	$\exp(\tau/2\tau_l) \times \{1 - \operatorname{erf}\sqrt{\tau/2\tau_l}\}$
Conformational fluctuation of the 'tube'	τ_r	a_2	$\sim M^3$	$\exp(-\tau/\tau_r)$

(a_0+a_1) and a_2 are the fractions of the normalized correlation function due to anisotropic segment re-orientation and the two secondary processes, respectively. The anisotropic segment re-orientation has been assumed for simplicity to be composed of two contributions only instead of a multicomponent distribution[4,6]. They arise from motions faster than our highest frequency (so that always $\omega\tau_0 \ll 1$) and from those which are accessible in our frequency range (so that the condition $\omega\tau_s \approx 1$ can be achieved). The fractions are a_0 and a_1, respectively.

This formalism has been applied to poly(ethylene oxide)[8] and polyethylene[9] melts. While the T_1 dispersion in a broad frequency range (10^3 to 10^8 Hz) could be described satisfactorily, there remained certain difficulties with the transverse relaxation. Non-exponential relaxation decays[1,2,10] have been observed and the motional narrowing limit[11] is no more valid for chain lengths exceeding a certain value. Thus relaxation theories of the BPP - type[11] are not suitable for the description of the transverse relaxation[8].

A more appropriate approach is the Anderson–Weiss formula[12] for the normalized envelope curve of the free induction decay:

$$g(t)=\exp\left(-M_2'\int_0^t (t-\tau)\, G_\omega(\tau)\, d\tau\right) \qquad (3)$$

M_2' is the second moment of the rigid lattice line (in square circular frequency units), $G_\omega(\tau)$ is the correlation function of the local resonance frequency. This formula is valid for a Gaussian distribution of the resonance frequencies at all times. Below, $G_\omega(\tau)$ will be equated with the correlation function $G(\tau)$ relevant for the spin lattice relaxation, so that longitudinal and transverse relaxation data can be simultaneously compared with the model. As the transverse relaxation is especially sensitive to all frequencies below 10^4 Hz, we have thus effectively an extension of the T_1 frequency range. (The limits of the so-called field-cycling technique which stands behind this range are discussed in ref. 13.)

The consideration of all these experimental data is essential for an unambiguous test of the model and the reliable determination of the parameters (*Table* 1). These quantities allow certain conclusions concerning the microstructure in melts. We have discussed[7,9] a procedure to estimate the correlation length of the conformation by combining data of the diffusion coefficient with relaxation parameters.

EXPERIMENTAL

Above 20 MHz, a conventional pulse spectrometer (Bruker SXP 4 - 100) with a shimmed high-resolution magnet (B - E 38) has been used. For the low-frequency range (10^4 to 2×10^7 Hz), a special field-cycling spectrometer has been constructed[14]. A cross-section of the high-temperature probehead of this apparatus is shown in *Figure* 1. The sample volume was about 1 cm^3.

In the case of the field-cycling measurements, the signals were rectified by diodes. The linearity of the whole receiver system was tested to ensure that no essential deviations have affected our results. All transverse relaxation decays have been measured by phase sensitive signal detection. The measuring errors were for the pure samples less than 10% and for the mixtures less than 30% at the lowest frequencies, i.e. in the worst case.

Table 2 characterizes the fractions of linear polyethylene (PE or PEH) and perdeuterated polyethylene (PED) used in this paper. The molecular weight distributions (*Figure* 2) have been measured by gel permeation chromatography. All samples have been evacuated for hours before the first melting, and all investigations have been carried out in the evacuated state (10^{-3} mm Hg).

The mixtures have been prepared by thoroughly mixing the powders. After degassing the samples, they were annealed in the molten state for several hours. This procedure turned out to be preferable to mixing the

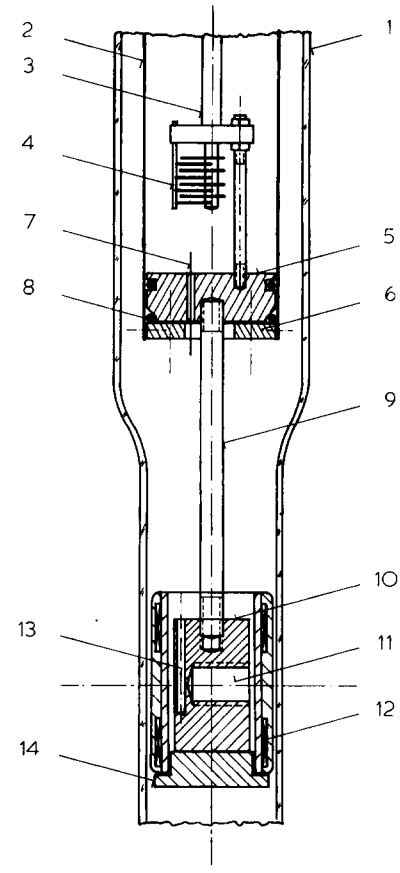

Figure 1 Cross-section through the high-temperature probehead of our field-cycling apparatus. 1, evacuable glass tube; 2, thin-walled brass tube fixed in the glass tube by the aid of a metal/glass grinding; 3, poly(vinyl chloride) tube including the tuning rod of the capacitor 4, capacitor; 5, and 6, vacuum seals; 7, bushings; 8, O-rings; 9, glass fibre rod; 10, sample holder; 11, RF-coil; 12, heater with ceramic coating; 13, temperature sensor; 14, cover of the heated volume

Table 2 Characterization of the samples used in this study

Sample	M_n	M_w/M_n	Supplier
1	2200	1.11	Polymer Laboratories (RAPRA) Shrewsbury, UK
2	5000	1.44	gift from Hüls AG, Marl, FRG
3	9600	1.38	fractionated from Lupolen 6011 L
4	84 000	1.10	supplied by Knauer, West-Berlin
5	100 000	1.25	fractionated from Lupolen 6011 L
6	180 000	2.4	Merck AG, Darmstadt, FRG

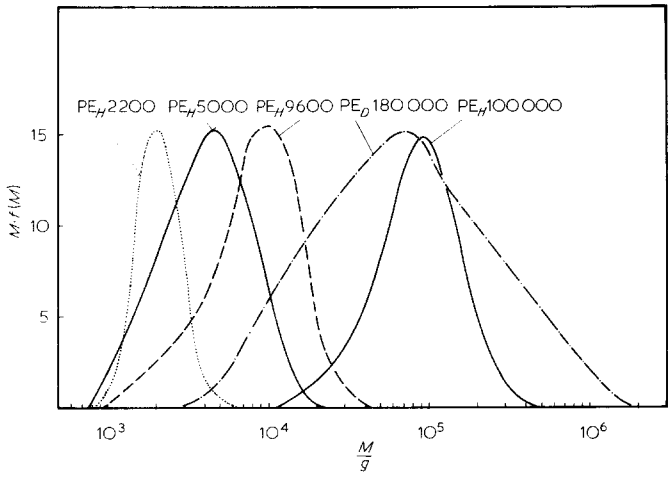

Figure 2 Gel permeation chromatography (g.p.c.) curves of the samples investigated in this work. The proper distribution function of the molecular weights is $f(M)$

polymers in solutions. In that case, a phase separation occurred due to the different solubilities for different chain lengths. The homogeneity of the mixtures could be controlled by the exponential decay of the longitudinal relaxation curve. The perdeuterated polyethylene (PED) yielded no detectable proton signal under the measuring conditions of our experiments.

LONGITUDINAL RELAXATION

The T_1 dispersion data of four different polyethylene fractions are given in *Figures* 3 and 4. Although the different molecular weight dependences and the different time scales of the three components would allow the theoretical curves to fit these data, it was desirable to have a direct access to the individual components.

Two of the components, namely the anisotropic segment re-orientation and the longitudinal chain diffusion are governed by intramolecular kinetics. The conformational fluctuation, however, is an intermolecular effect, so that this component can be influenced by the choice of the sample constitution[15]. The observation of the proton relaxation of chains with a molecular weight M_1 in a matrix of deuterated chains with a molecular weight M_2 leads to a longitudinal chain diffusion component determined by $\tau_l = \tau_l(M_1)$ and to tube fluctuations determined by $\tau_r = \tau_r(c, M_1, M_2)$. c is the ratio of mixture.

Figures 5 and 6 show the result of this experiment. Clearly the predictions of the three-component model are fulfilled in the sense that the tube fluctuation of the short chains is now modified according to the large molecular weight of the matrix. In other words, the low-frequency plateau of the mixture is shifted outside the accessible frequency range.

The solid lines in *Figures* 3 to 6 are fitted by a least squares procedure with a single set of parameters given in *Table* 3. The activation energy of the elementary process is given by that of the γ-process in amorphous polyethylene, i.e. by 27.8 kJ/mol[14].

For the mixtures we had to assume that the τ_r values are at least 70 times the τ_r value of the pure short chain material in order to describe the low-frequency dependence of T_1. The molecular weight distributions (*Figure* 2) have also been taken into account. It turned out that they have no essential influence on T_1 in the frequency range investigated in this paper. Merely in the region $\omega\tau_r \approx 1$ the curves are expected to be affected by these distributions. A stronger effect of the molecular weight distribution is observed in the case of the transverse relaxation as shown in the next section.

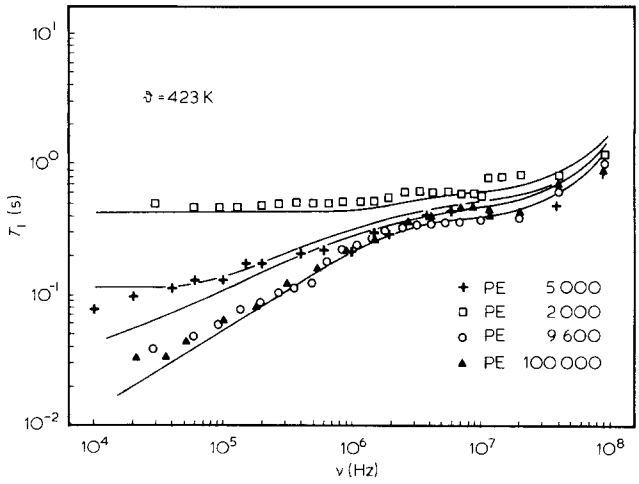

Figure 3 T_1 dispersion of different PE fractions at 423 K. The solid lines are theoretical curves calculated with the parameters given in *Table 3*

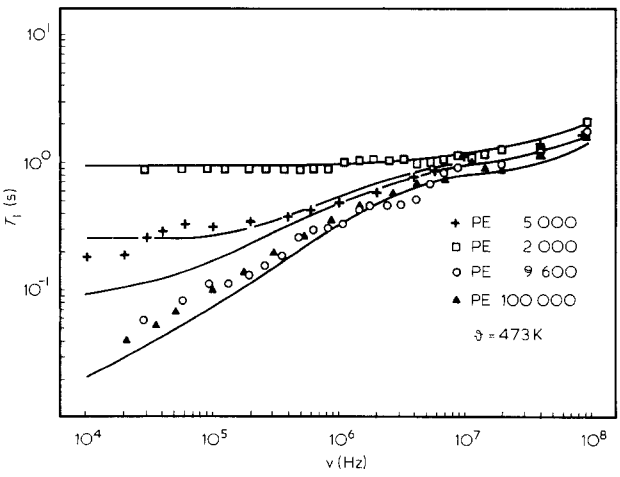

Figure 4 T_1 dispersion of different PE fractions at 473 K. The solid lines are theoretical curves calculated with the parameters given in *Table 3*

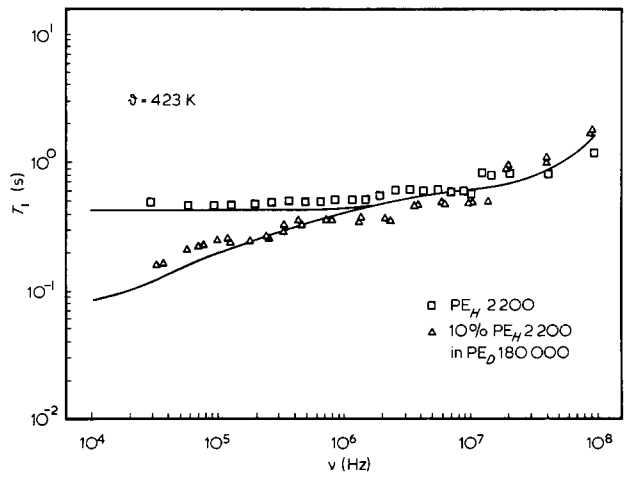

Figure 5 Comparison of the T_1 dispersion at 423 K of PEH 2200 with that of a mixture 10% by weight PEH 2200 in PED 180 000. The solid lines are calculated with the parameters given in *Table 3*

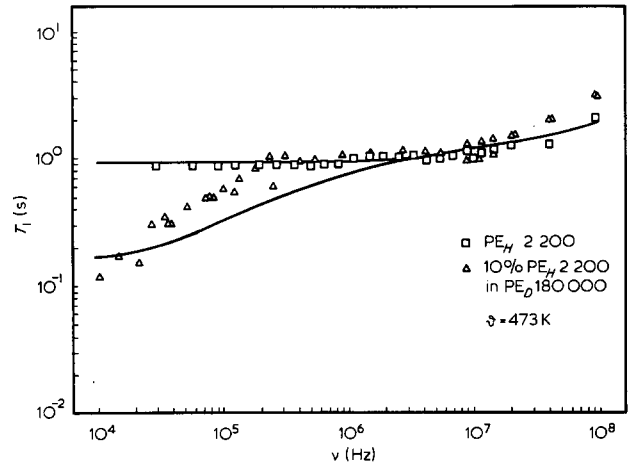

Figure 6 Comparison of the T_1 dispersion at 473 K of PEH 2200 with that of a mixture 10% by weight PEH 2200 in PED 180 000. The solid lines are calculated with the parameters given in *Table 3*

Table 3 Parameters fitted to the experimental data. All theoretical curves have been calculated on the basis of this set

	200°C	150°C
τ_s [s]	$6.4 \times 10^{-10} \pm 20\%$	
τ_l [s]	$2.3 \times 10^{-13} \times M \pm 30\%$	$2.3 \times \tau_{s,l,r}$ (200°C)
τ_r [s]	$3.5 \times 10^{-18} \times M \pm 40\%$	
$a_2 : a_1$	$5.8 \times 10^{-2} \pm 20\%$	
$a_0 : a_1$	$6.1 \pm 5\%$	

TRANSVERSE RELAXATION

Experimental Results

Transverse relaxation is of special interest with respect to the slow components of molecular motion. It will be shown that the time parameters of the secondary processes (τ_l and especially τ_r) determine the transverse relaxation behaviour. Thus we have a complementary method to the T_1 dispersion measurements, which is sensitive to the frequency range below 10^4 Hz.

We have investigated both the shape of the free induction decay (FID) and the transverse relaxation decay measured by the aid of the Carr–Purcell–Gill–Meiboom (CPGM) method[16]. The frequency was 90 MHz, the temperature 423 K. The samples were the same as used for the T_1 experiments (*Table* 2).

The experimental data are shown in *Figures* 7 and 8. Increasing molecular weights lead to faster decays both of the free induction signals and of the transverse relaxation curves. Moreover, short chains dissolved in a matrix of long (deuterated) chains show faster decays than in the bulk material. This means that transverse relaxation can be expected to be sensitive to the three components of molecular motion.

The experiments revealed two remarkable facts: (1) the relaxation curves obtained by the CPGM - sequence decay essentially slower than the *FID*, although the decay times should be comparable if the inhomogeneity of

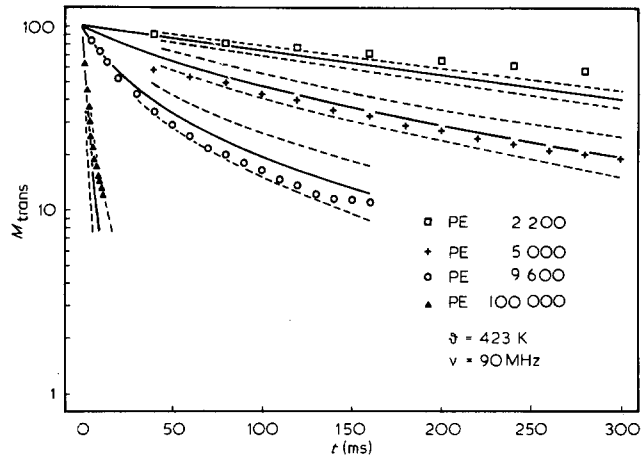

Figure 7 CPGM decays of various PE fractions at 423 K and 90 MHz. The solid lines are calculated with the parameters given in *Table 3* and the molecular weight distributions (*Figure 2*) by the aid of the Anderson–Weiss formula (equation 3). The broken lines indicate the range covered by the theoretical curve if an inaccuracy of ±5% in M_n is assumed

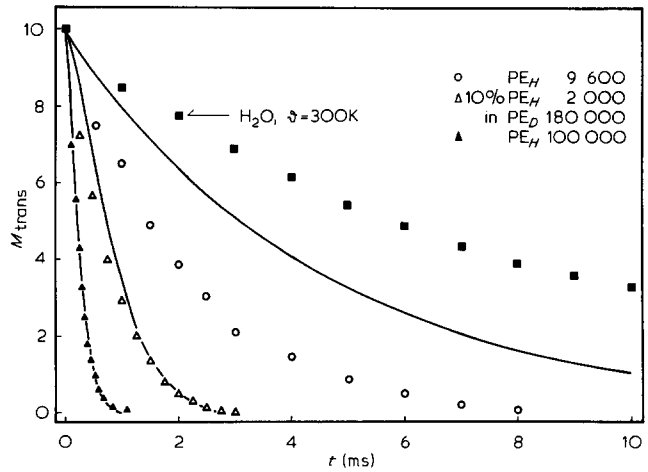

Figure 8 Free induction decays of various PE fractions at 423 K and 90 MHz. The FID of distilled water at 300 K is also shown in order to characterize the decay time of the spectrometer. The solid lines have been calculated with the parameters given in *Table 3* by the aid of the Anderson–Weiss formula (equation 3) and by setting $a_0 = 0$. Instead of the molecular weight distributions (*Figure 2*) we have used merely the M_n values. The deviation for PEH 9600 is already a consequence of the decay time intrinsic for the spectrometer

the magnet is negligible. This was at least the case for the PE fractions $M_n > 10^4$. The conclusion will be that an internal field inhomogeneity is produced in the samples; (2) the PE fractions of higher molecular weights (PE 5000, 9600 and 100 000) showed a non-exponential CPGM decay in contrast to the fraction of PE 2200 and the mixture of PE 2200 with PED 180 000. It will be shown that this is a consequence of the molecular weight distribution. (The longitudinal relaxation curves were exponential throughout. This can be understood as a consequence of spin diffusion[11].)

Field inhomogeneity in PE melts

The fact that the free induction signal decays essentially faster than the proper relaxation curve even when the inhomogeneity of the magnet was negligible, cannot be explained by dipolar broadening. In that case no echoes would occur with the CPGM-sequence (compare ref. 17). Therefore we have to discuss any type of internal field inhomogeneity, whose influence is reversibly inverted by the CPGM - sequence. The perturbation of the external magnetic field could have its origin in the macroscopic non-ellipsoidal shape of the sample, in molecular anisotropies such as the chemical shift and the susceptibility, and in microscopic inhomogeneities of the density caused by invisible voids.

The first possibility has been checked by annealing the samples at 150°C up to three weeks. (Longer annealing periods led to a strong influence of chain cracking.) All samples showed thereafter a cylindric, i.e. approximately an ellipsoidal shape. Nevertheless, no approach of the free induction and relaxation decays could be observed. Thus this argument is ruled out.

The anisotropy of the chemical shift covers a range of about 10^3 Hz for protons[18]. In other words, the motional narrowing is even more effective for the chemical shift distribution than for dipolar broadening, so that this explanation is already excluded by the argument, that dipolar broadening is not responsible for the discrepancy between free induction and relaxation decay.

The remaining type of field inhomogeneity is connected with an inhomogeneity in the density of the material and therefore in the susceptibility. We conclude that there are microscopic voids within the material causing differences in the magnetic susceptibility of about $\Delta\chi \approx 10^{-6}$. Such voids have also been detected by neutron scattering[19]. The field inhomogeneity caused by these voids depends on the shape. An estimation can be carried out for spheres (see Appendix). It turned out that the order of magnitude is insufficient for a complete explanation of this effect by spherical voids, but is expected to be sufficient for other shapes of the voids.

The dependence of the time scale of the free induction decay on the molecular weight is similar to that of the relaxation decay. The conclusion is that the field inhomogeneity is more or less averaged out depending on the speed of the diffusion of the voids. The diffusion of the voids, however, depends on the rate of the environmental rearrangement, i.e. on the parameter τ_r which is proportional to M^3 (*Table* 1). Thus it is plausible that both types of transverse signal decays depend in the same manner on the molecular weight.

Theoretical description of the transverse relaxation decay

The calculations are based on equation (3), where we have equated the correlation function $G_\omega(\tau)$ with $G(\tau)$ (equation 1).

The time constants defined in equation (1) for $G(\tau)$ are expected to be also relevant for $G_\omega(\tau)$, because both correlation functions depend on the same fluctuations, namely those of the dipolar interaction. There might be, however, certain differences in the distribution of the amplitudes a_j of the individual components because different terms of the dipolar Hamiltonian are responsible for the longitudinal and transverse relaxation, respectively[11]. As transverse relaxation is dominated by the slowest components, we conclude that the use of identical amplitudes is nevertheless a good approximation.

For the second moment we have used $M_2' = \gamma^2\ 1.93 \times 10^{-7}\ T^2$ which corresponds to the rigid lattice value for an isolated chain. (γ is the magnetogyric ratio of protons.) The neglect of the intermolecular contribution is plausible because of the volume expansion at the melt transition and is necessary because no exact value for melts is available.

The numerical evaluation of equation (3) in combination with equation (1) leads to some difficulties: $(1 - \mathrm{erf}\, x)$ is less than 10^{-150} for $x > 18.5$ while our computer works only in the range of 10^{-150} to 10^{+150}. We therefore calculated the function $e^x(1 - \mathrm{erf}\ \sqrt{x})$ by the series expansion[20]:

$$e^x(1-\mathrm{erf}\sqrt{x}) = \frac{1}{\pi}\sum_{k=0}^{n-1}\frac{(-1)^k\Gamma(k+0.5)}{x^{k+0.5}} - \frac{1}{\pi}R_n \qquad (4)$$

where

$$|R_n| < \frac{\Gamma(n+0.5)}{|x|^{n+0.5}}$$

and $\Gamma(\ )$ is the gamma-function. For large values of x this series converges very quickly so that only a few terms are needed.

The experiments could not be described satisfactorily without taking into account the distributions of molecular weight. Better results can be obtained by considering the distributions shown in *Figure* 2. For a numerical treatment we have approximated the distribution function by a step function with about 30 discrete values. This means that we have to deal now with a mixture of 30 different portions of different molecular weight. We calculated the transverse relaxation decay for each molecular weight and took the average of them by the aid of the weighting factors given by the step distribution function. *Figure* 9 shows the influence of the molecular weight distribution.

It should be noted that this procedure is a rough approximation as we supposed, that there are different parts of the sample with the same molecular weight. In reality the relaxation of a reference chain is influenced both by long and short neighbouring chains. Nevertheless, this approximation describes quite successfully the experimental data and experimental confirmation of this can also be found in ref 23. The shape of the distribution of M can reliably be determined by the aid of gel permeation chromatography in contrast to the absolute value of M_n, which can only be gauged within $\pm 10\%$. The experimental curves in *Figure* 7 are therefore completely described within these limits. The relaxation curves of the mixture PEH 2200 in the deuterated matrix PED 180 000 are also compatible with the τ_r values used for the description of the T_1 dispersion. *Table* 4 shows the comparison between theory and experiment. Altogether

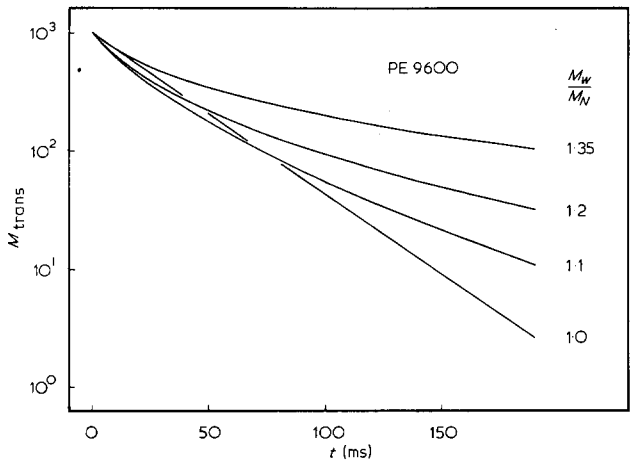

Figure 9 CPGM decays calculated for a molecular weight M_n = 9600. In order to show the influence of the molecular weight distribution, we have artificially varied the width (i.e. M_W/M_n) of the measured distribution given in *Figure 2* for PE 9600. The shape of the distribution remained unaffected. It is shown that the deviation from an exponential decay depends strongly on M_W/M_n

we can state that the transverse relaxation behaviour is strongly affected by the fluctuation of the tube characterized by the parameter τ_r.

Theoretical description of the free induction decay

As outlined above, there should be a magnetic field inhomogeneity caused by voids in the material. This inhomogeneity effect dominates the free induction decay for large molecular weights. The diffusion of the voids is then slow enough, so that this broadening effect is not averaged out. The diffusion of the voids is a consequence of the network dynamics. Thus it is plausible that τ_r is again the most important parameter. As the diffusion of voids is simultaneously influenced by many chains, the molecular weight distribution is no more relevant and the number-average molecular weight, M_n should be used in the calculations. It is then no bad approximation to use equation (1) for the effective correlation function by simply assuming $a_0 = 0$. *Figure* 8 shows the comparison with the experiments. The coincidence is satisfactory except for $M_n < 9600$ where the influence of the inhomogeneity of the external magnetic field becomes relevant.

The fact that the influence of the deuterated matrix on the free induction decay is very different from that on the CPGM - decay (*Table* 4), indicates that these curves show a different dependence on the network dynamics: The *FID* of the mixture could only be described by taking into account the τ_r value corresponding directly to $M_n = 180\ 000$ instead of the value fitted to the T_1 dispersion and the CPGM - decay.

DISCUSSION OF RELEVANT NETWORK PROPERTIES

We have shown that molecular fluctuations in polymer melts can be described by three components so far they concern the upper frequency range which is accessible by longitudinal relaxation and very low frequencies relevant for transverse relaxation. The molecular weight dependence of the measured quantities could be related to that of microscopic parameters. The coincidence of theory and experiments is satisfactory at least in the light of the diverse simplifications in the theoretical treatment and of the imponderabilities connected with the different polyethylene samples[21]. One point needs, however, thorough discussion: in which way do the network dynamics determine the local conformation of the surrounding tube?

Mixtures of different chain lengths show a correlation time of the local tube fluctuation $\tau_r = \tau_r(c, M_1, M_2)$, where M_1 and M_2 are the molecular weights of the two constituents and c is the ratio of mixture. The dependence on *both* molecular weights and on the ratio of mixture became clear, at least for $M < M_{crit}$, where M_{crit} corresponds to the so-called entanglement length.

An estimation[9] suggests that the local tube conformation is determined by at least three chains. Thus it is plausible that both chain lengths of a mixture are relevant for the tube fluctuation. On the other hand, it can be imagined that the tube conformation is altered even in a rigid network when the reference chain is threaded around different netpoints while diffusing forth and back[22]. One could therefore expect that merely the molecular weight of the observed chains is relevant for the tube fluctuation especially if the matrix consists of very long chains.

The τ_r value of PEH 2200 dissolved in a PED 180 000 matrix, however, was found to be influenced by the (quasi-rigid) matrix. So we have to assume that the tube conformation can already be altered *before* the chain is completely threaded around other netpoints at least for $M < M_{crit}$.

The problem is now to find a quantitative treatment of the influence of the long-chain matrix on the tube fluctuation of the short chains. The solution requires more detailed informations concerning the functional relationship $\tau_r = \tau_r(c, M_1, M_2)$, which are not yet available. For the moment therefore we want to try a simple consideration.

We assume that the correlation time τ_r of the tube fluctuation is proportional to the mean lifetime τ_n of one of the chain contacts relevant for the local conformation of the reference tube. This means that the netpoint does not necessarily involve the reference chain. A netpoint links two chains for a certain time, so that there are two limiting cases. The mean lifetime τ_n might be given either by the mean diffusion time which only *one* chain needs to leave the chain contact via reptation, or by the time required until *both* chains have diffused out of the netpoint environment, so that any recombination at this place becomes improbable immediately afterwards.

Table 4 Comparison of the experimental and calculated decay times to $M_{trans}(0)/e$ both for the CPGM–decay and the *FID*

Sample	Decay time to $1/e\ M_{trans}(0)$ in (ms)			
	CPGM		*FID*	
	Exp.	Calc.	Exp.	Calc.
PE 2200	540 ± 5%	330		44
PE 5000	200 ± 5%	218		14
PE 9600	36 ± 10%	44	2.16 ± 10%*	4.33
PE 100 000	3.5 ± 10%	2	0.3 ± 10%	0.3
10% PEH 2200 in PED 180 000	260 ± 10%	68†	0.76 ± 10%	0.96

* Influenced by the decay time of the apparatus
† Calculated without taking into account the distributions of molecular weights

In the first limit we have an average disentanglement rate of a chain contact (calculated by assuming Poisson statistics for simplicity):

$$\frac{1}{\tau_n^m}=p_{11}\frac{2}{\tau_{rep}(M_1)}+2p_{12}\left(\frac{1}{\tau_{rep}(M_1)}+\frac{1}{\tau_{rep}(M_2)}\right)+p_{22}\frac{2}{\tau_{rep}(M_2)} \tag{5}$$

where the index m refers to mixture and $p_{12}=p_{21}$. p_{ij} is the probability that a definite netpoint consists of two chains with the molecular weights M_i and M_j. $\tau_{rep}(M_i)$ is the mean reptation time the whole chain with the molecular weights M_i needs to leave the contact regions. For $M_2 \gg M_1$ we have:

$$\frac{1}{\tau_n^m}\approx(2p_{11}+2p_{12})\frac{1}{\tau_{rep}(M_1)} \tag{6}$$

compared with a disentanglement rate in the pure melt:

$$\frac{1}{\tau_n^p}=\frac{2}{\tau_{rep}(M_1)} \tag{7}$$

where the index p refers to pure melt. In the experiment discussed above, the ratio of mxiture was $c=10\%{:}90\%$, or $p_{11}=0.01$, and $p_{12}=0.09$. Consequently $\tau_n^m/\tau_n^p=10$.

The second limit where both entangled chains have to diffuse away can be treated by writing down the probability $W_{ij}(t)$ that a netpoint consisting of two chains with molecular weights M_i and M_j has been disentangled in the period $0\ldots t$

$$W_{ij}(t)=(1-e^{-t/\tau_{rep}(M_i)})(1-e^{-t/\tau_{rep}(M_j)}) \tag{8}$$

where we have again assumed Poisson statistics for simplicity. The probabilities that the netpoints will be disentangled between t and $t+dt$ are then $\dot{W}_{ij}\,dt$, so that we have a mean lifetime of the contacts:

$$\int_0^\infty t'\dot{W}_{ij}(t')dt'$$

The average disentanglement rate is then for the mixture:

$$\frac{1}{\tau_n^m}=\frac{p_{11}}{\int_0^\infty t'\dot{W}_{11}(t')\,dt'}+\frac{2p_{12}}{\int_0^\infty t'\dot{W}_{12}(t')\,dt'}+\frac{p_{22}}{\int_0^\infty t'\dot{W}_{22}(t')\,dt'}$$

$$=\frac{2}{3}p_{11}\frac{1}{\tau_{rep}(M_1)}+\frac{2}{3}p_{22}\frac{1}{\tau_{rep}(M_2)}+$$

$$\frac{2p_{12}}{\tau_{rep}(M_1)+\tau_{rep}(M_2)-\{\tau_{rep}(M_1)^{-1}+\tau_{rep}(M_2)^{-1}\}^{-1}} \tag{9}$$

For $M_2 \gg M_1$ or $\tau_{rep}(M_2) \gg \tau_{rep}(M_1)$ we have:

$$\frac{1}{\tau_n^m}\approx\frac{2}{3}p_{11}\frac{1}{\tau_{rep}(M_1)} \tag{10}$$

Compared with a disentanglement rate in the pure melt

$$\frac{1}{\tau_n^p}=\frac{2}{3}\frac{1}{\tau_{rep}(M_1)} \tag{11}$$

For the conditions of our experiments this means a ratio:

$$\tau_n^m/\tau_n^p=\frac{1}{p_{11}}=100$$

The reality should lie between these limits so that we have to discuss the range:

$$10\leqslant\tau_n^m/\tau_n^p\leqslant 100 \tag{12}$$

for the present example, i.e. with $\tau_r\sim\tau_n$

$$10\leqslant\tau_r^m/\tau_r^p\leqslant 100 \tag{13}$$

In other words, the value 70 for this ratio which has been used above for the description of the T_1 dispersion and the transverse relaxation turns out to be quite reasonable.

It is also plausible that the free induction decay of the mixture could only be described by a τ_r value corresponding to the molecular weight of the deuterated matrix alone, while the transverse relaxation measured with the CPGM - sequence is again compatible with an increase of τ_r by a factor ≈ 70. The reason is that void diffusion requires the simultaneous disentanglement of several net-points while tube fluctuation is initiated by the loosening of one out of several relevant chain contacts.

A second point we should mention is the inhomogeneity effect which we have tried to explain by the occurrence of voids. The question is whether we have to deal with an equilibrium property or not. Although there are several hints that this effect can be observed also with other polymers and with different preparation methods, we are not able to give a final answer. More detailed investigations will be necessary for a classification of this situation. Furthermore the influence of M_{crit} has to be discussed and a preliminary investigation will be published elsewhere[24].

ACKNOWLEDGEMENTS

This work has been supported by Deutsche Forschungsgemeinschaft. We are indebted to Chemische Werke, Hüls A. G., for the gift of one polyethylene fraction and Dr I. Asbach, Universität Ulm for carrying out the g.p.c. measurements. Helpful discussions with Drs. A. Peters and G. Voigt are also acknowleged.

REFERENCES

1 McCall, D. W., Douglass, D. C. and Anderson, E. W. *J. Polym. Sci.* 1962, **59**, 301
2 Preissing, G. and Noack, F. *Progr. Colloid Polym. Sci.* 1975, **57**, 216
3 Lindberg, J. J., Sirén, J., Rahkamaa, E. and Törmälä, P. *Angew. Makromol. Chem.* 1976, **50**, 187

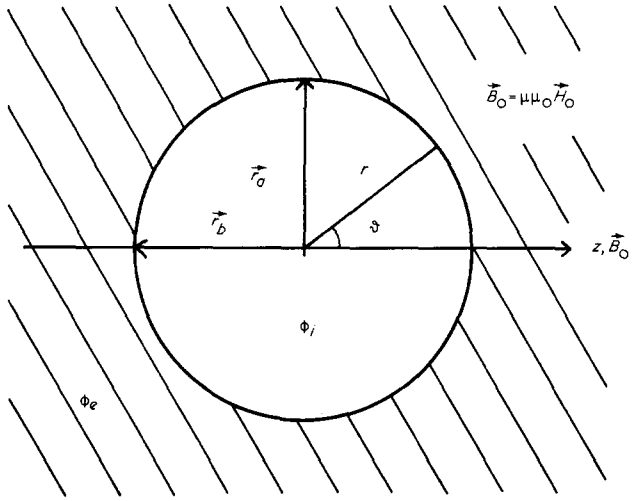

Figure 10 Cross-section of the spherical void assumed for the estimation of the inhomogeneity effect

4 Kimmich, R. *Polymer* 1977, **18**, 233
5 de Gennes, P. G. *J. Chem. Phys.* 1971, **55**, 572
6 Kimmich, R. and Doster, W. *J. Polym. Sci. (Polym. Phys. Edn)* 1976, **14**, 1671
7 Kimmich, R. *Polymer* 1975, **16**, 851
8 Kimmich, R. and Schmauder, Kh. *Polymer* 1977, **18**, 239
9 Kimmich, R. and Koch, H. *Colloid Polym. Sci.* 1980, **258**, 261
10 Gölz, W. L. F. and Zachmann, H. G. *Makromol. Chem.* 1975, **176**, 2721
11 Abragam, A. 'The Principles of Nuclear Magnetism', Oxford University Press, Oxford, 1961
12 Anderson, P. W. *J. Phys. Soc. Japan* 1954, **9**, 316
13 Kimmich, R. *Bull. Magn. Reson.* in press
14 Voigt, G. and Kimmich, R. 1980, **21**, 1002
15 Koch, H. and Kimmich, R. *Polymer* 1979, **20**, 132
16 Farrar, T. C. and Becker, E. D. 'Pulse and Fourier Transform NMR', Academic Press, New York, 1971
17 Cohen-Addad, J. P. and Vogin, R. *Phys. Rev. Lett.* 1974, **33**, 940
18 Haeberlen, U. 'High Resolution NMR in Solids', Academic Press, New York, 1976
19 Pechhold, W. and Sautter, E. personal communication
20 Gradshteyn, I. S. and Ryzhik, I. M. 'Table of Integrals, Series and Products', Academic Press, New York, 1965
21 Folland, R. and Charlesby, A. *Eur. Polym. J.* 1979, **15**, 953
22 de Gennes, P. G. *Macromolecules* 1976, **9**, 594
23 Shevelev, V. A., Belov, G. P., Platonov, M. P. and Jadra, E. R. *Vysokomol. Soed.* USSR 1976, **A1813**, 625
24 Koch, H., Bachus, R. and Kimmich, R. *Bull. Magn. Res.* in press

APPENDIX

Magnetic field inhomogeneity caused by microscopic voids:

We have calculated the inhomogeneity caused by a spherical void (radius b) in a medium of relative permeability μ(*Figure* 10). The starting point for these considerations are the Maxwell equations for the magnetic flux density $\vec{B}$ and the magnetic field strength $\vec{H}$ div $\vec{B}_0 = 0$ and rot $\vec{H}_0 = 0$ in absence of any currents. This means that the flux density $\vec{B}_0 = \mu_0\mu\vec{H}_0$ can be derived from a magnetic potential φ, which satisfies Laplace's equation:

$$\Delta\varphi = 0 \quad \text{or} \quad \vec{B}_0 = \mu_0\mu \text{ grad } \varphi \tag{14}$$

For the potential φ in an external flux density $\vec{B}_0 = (0,0,B_0)$ we make the following relation which automatically satisfies Laplace's equation (compare *Figure* 10):

$$r > b: \quad \varphi_e = -B_0 r\cos\theta + \sum_{l=0}^{\infty} \frac{\alpha_l}{r^{l+1}} p_l(\cos\theta) \tag{15a}$$

$$r < b: \quad \varphi_i = \sum_{l=0}^{\infty} \beta_l r^l p_l(\cos\theta) \tag{15b}$$

$p_l(\cos\theta)$ are the Legendre polynomials. The coefficients α_l and β_l can by calculated by the aid of the boundary conditions for $\vec{H}_0$ and $\vec{B}_0$. This leads to:

$$\varphi_e = -B_0 r\cos\theta - \frac{1}{r^3}\frac{\mu-1}{2\mu+1} b^3 B_0 r\cos\theta \tag{16a}$$

$$\varphi_i = -\frac{3\mu}{2\mu+1} B_0 r\cos\theta \tag{16b}$$

and correspondingly to:

$$B_{e,z} = \mu B_0 + \frac{\mu-1}{2\mu+1} b^3 B_0 \left(\frac{1}{r^3} - \frac{3z^2}{r^5}\right) \tag{17a}$$

$$B_{i,z} = \frac{3\mu}{2\mu+1} B_0 \tag{17b}$$

The maximum difference of the magnetic field in z-direction outside of the sphere is then given by (*Figure* 10)

$$\Delta B_e = B_e(\vec{r}_a) - B_e(\vec{r}_b) = \mu\frac{\mu-1}{2\mu+1} B_0 \tag{18}$$

with $\mu = 1+\chi$. Typical values are $B_0 \approx 2T$ and $\chi \approx -10^{-6}$ so that $\Delta B \approx 2\times10^{-6}$ T. The difference in the proton Larmor frequency is then $\Delta\omega = 2\pi \cdot 80$ Hz. These values show that although the influence of spherical voids is not negligible, it is not able to explain the observed inhomogeneity effect in its full extent.